

Supporting Information

Synthesis and evaluation of four novel nitrogen-heterocyclic ruthenium polypyridyl complexes as photosensitizers for one and two-photon photodynamic therapy

Junfeng Kou,^{*a} Jinchao Shen,^b Mingwei Lin,^b Kai Xiong,^b Lili Wang,^b Fangmian Wei,^b Junfeng Zhang^a

a. College of Chemistry and Chemical Engineering, Yunan Normal University, Kunming, 650500, P. R. China Email: kjf416@163.com

b. MOE Key Laboratory of Bioinorganic and Synthetic Chemistry, School of Chemistry, Sun Yat-Sen University, Guangzhou 510275, P. R. China.

Table of Contents

Synthesis	1
Scheme S1.....	1
Supporting Figures and Tables	2
Fig. S1	2
Fig. S2	3
Fig. S3	4
Fig. S4.....	5
Fig. S5	6
Fig. S6.....	7
Fig. S7	8
Fig. S8.....	9
Table. S1	10
Fig. S9.....	10
Fig. S10.....	10
Fig. S11	11
Fig. S11	11
References.....	11

Synthesis of pyrazolyl aldehydes (o-ppzCHO, o-ppCHO, m-ppCHO and p-ppCHO)¹

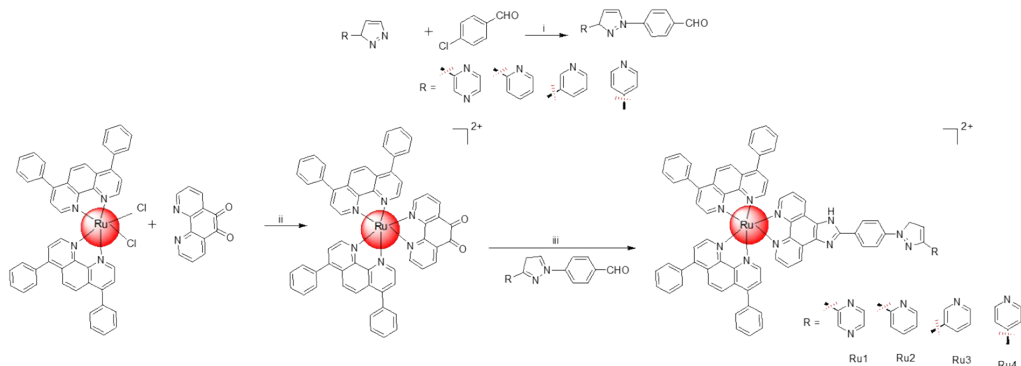
2-(4H-pyrazol-3-yl) pyrazine (1mmol, 146 mg), 2-(4H-pyrazol-3-yl)pyridine (1 mmol, 145 mg), 3-(4H-pyrazol-3-yl) pyridine (1mmol, 145 mg) or 4-(4H-pyrazol-3-yl) pyridine (1mmol, 145 mg), 4-chlorobenzaldehyde(1mol, 140mg), KOH (2.5 mmol, 140 mg). A pressure tube was charged with the corresponding nitrogenated heterocycle (1), KOH (2.5 mmol, 140 mg), and dry DMSO (1.5 mL) under argon atmosphere. The resulting mixture was stirred in an oil bath at 120 °C until the end of the reaction. The mixture was quenched with a saturated solution of NH₄Cl and extracted with ethyl acetate (2x10 mL). The organic phase was dried over MgSO₄, followed by evaporation under reduced pressure to remove the solvent. The product was purified by column chromatography on silica gel (decreasing hexane/ethyl acetate ratio). as the eluent. All the compounds were further characterized by LC-MS, 1H NMR and elemental analysis.

o-ppzCHO Yield: 0.15g, 80%. ESI-MS [m/z]: 251.15. ¹H NMR (400 MHz, DMSO-d₆) δ 10.05 (s, 1H), 9.42 - 9.30 (m, 1H), 8.85 (d, *J* = 2.8 Hz, 1H), 8.77- 8.62 (m, 2H), 8.23 (d, *J* = 8.4 Hz, 2H), 8.10 (d, *J* = 8.2 Hz, 2H), 7.25 (d, *J* = 2.9 Hz, 1H).

o-ppCHO Yield: 0.19g, 76%. ESI-MS [m/z]: 250.14. ¹H NMR (400 MHz, DMSO-d₆) δ 10.02 (s,1H), 8.78-8.77 (d,1H), 8.64-8.63 (m,1H), 8.20-8.17 (d, 2H), 8.12-8.10 (d, 1H), 8.07(d, 2H), 7.92-7.87 (td, *J* = 7.7, 1H), 7.40-7.37 (m,1H), 7.17-7.16 (d,1H). ¹H NMR (400 MHz, DMSO-d₆) δ 10.02 (s, 1H), 8.77 (d, *J* = 2.6 Hz, 1H), 8.67 – 8.60 (m, 1H), 8.19 (d, *J* = 8.5 Hz, 2H), 8.12 (s, 1H), 8.06 (d, *J* = 8.5 Hz, 2H), 7.90 (td, *J* = 7.7, 1.8 Hz, 1H), 7.43 –7.33 (m, 1H), 7.16 (d, *J* = 2.6 Hz, 1H).

m-ppCHO Yield: 0.18g, 72%. ESI-MS [m/z]: 250.15. ¹H NMR (400 MHz, DMSO-d₆) δ 10.09-10.00 (m, 1H), 9.24- 9.14 (m, 1H), 8.81 (q, *J* = 2.7 Hz, 1H), 8.60 (dd, *J* = 4.8, 1.5 Hz, 1H), 8.33 (dq, *J* = 8.0, 2.1 Hz, 1H), 8.24 - 8.14 (m, 2H), 8.12 - 8.03 (m, 2H), 7.51 (ddt, *J* = 8.6, 4.5, 1.9 Hz, 1H), 7.27 (q, *J* = 2.5 Hz, 1H).

p-ppCHO Yield: 0.16g, 64%. ESI-MS [m/z]: 250.14. ¹H NMR (400 MHz, DMSO-d6) δ 10.02 (s, 1H), 8.82 (d, *J* = 2.7 Hz, 1H), 8.65 (d, *J* = 6.1 Hz, 2H), 8.18 (d, *J* = 8.7 Hz, 2H), 8.07 (d, *J* = 8.7 Hz, 2H), 7.91 (d, *J* = 6.1 Hz, 2H), 7.31 (d, *J* = 2.6 Hz, 1H).



Scheme S1. Synthetic routes for Ru1-Ru4. (i) KOH, dry DMSO under argon atmosphere in an oil bath at 120°C. (ii) CH₃OH/H₂O 1:1, reflux, 3h. (iii) AcOH, reflux, 12h

Supporting Figures and Tables

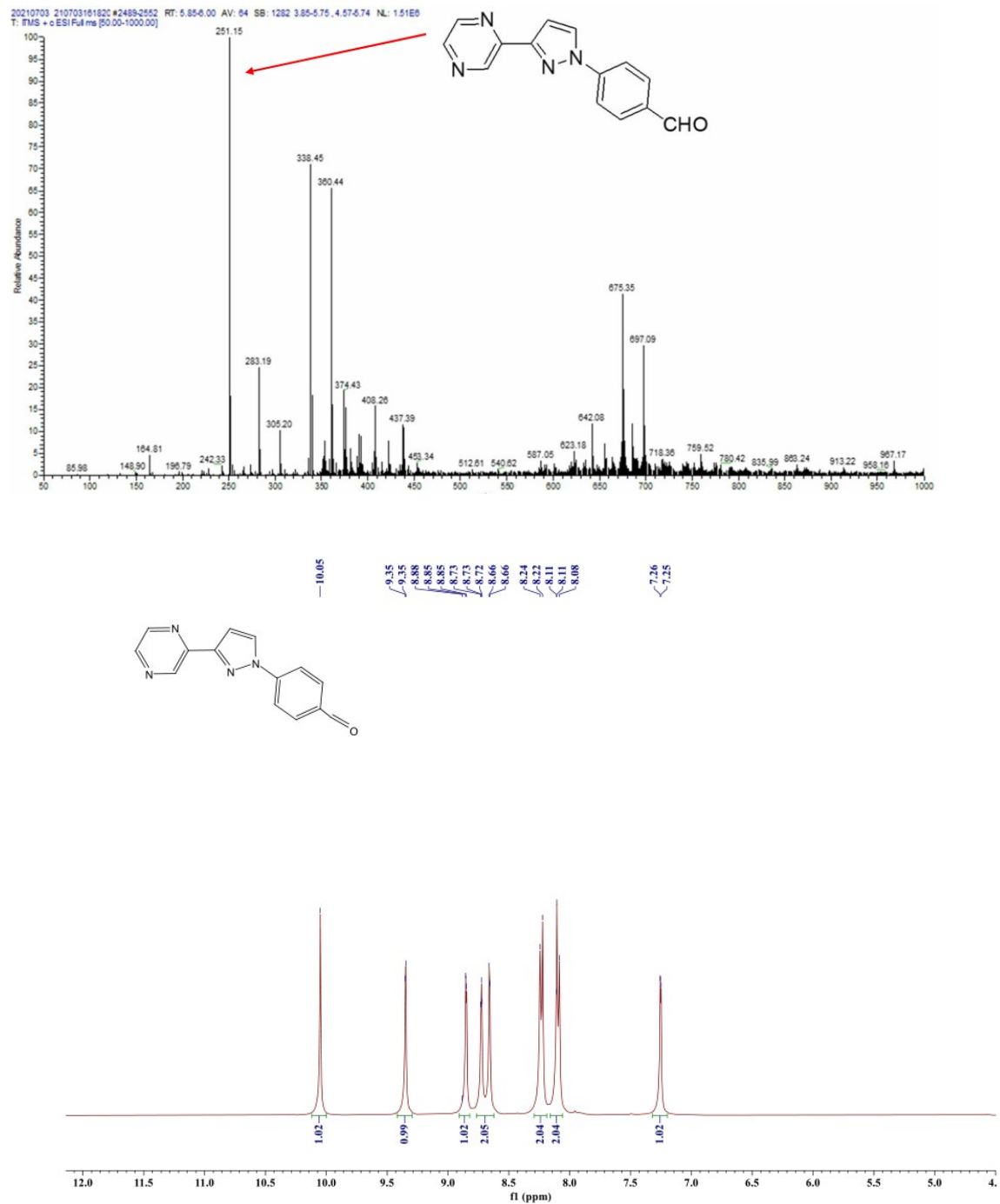


Fig. S1 ESI-MS spectrum, ^1H NMR spectrum of o-ppzCHO

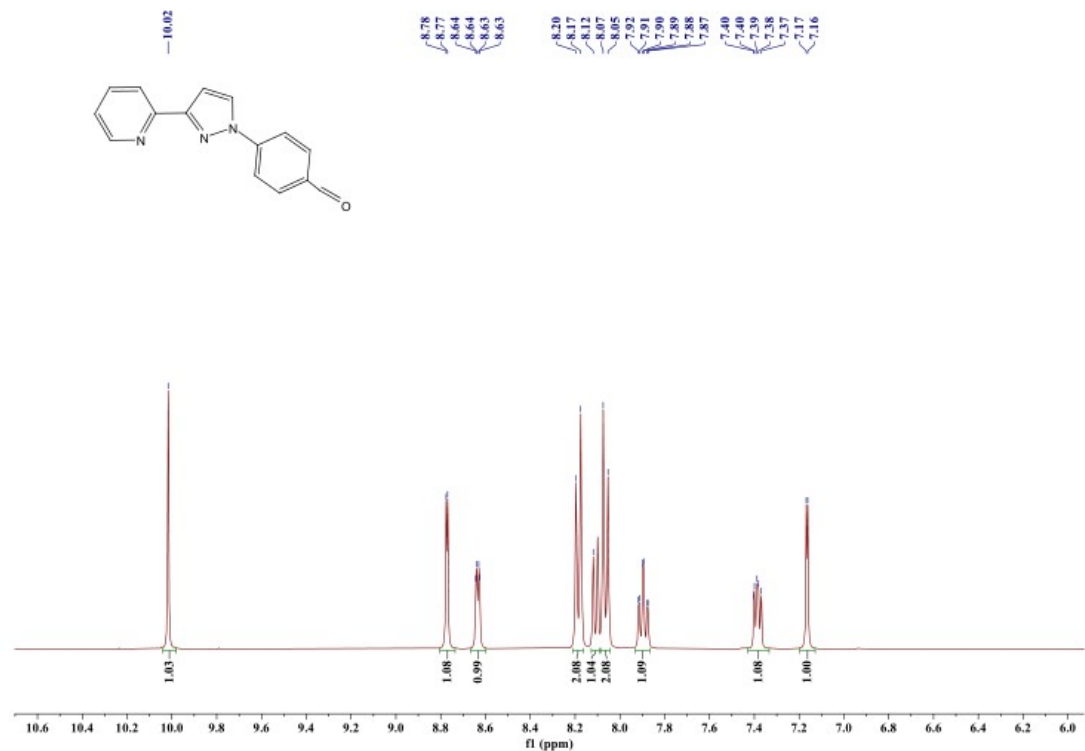
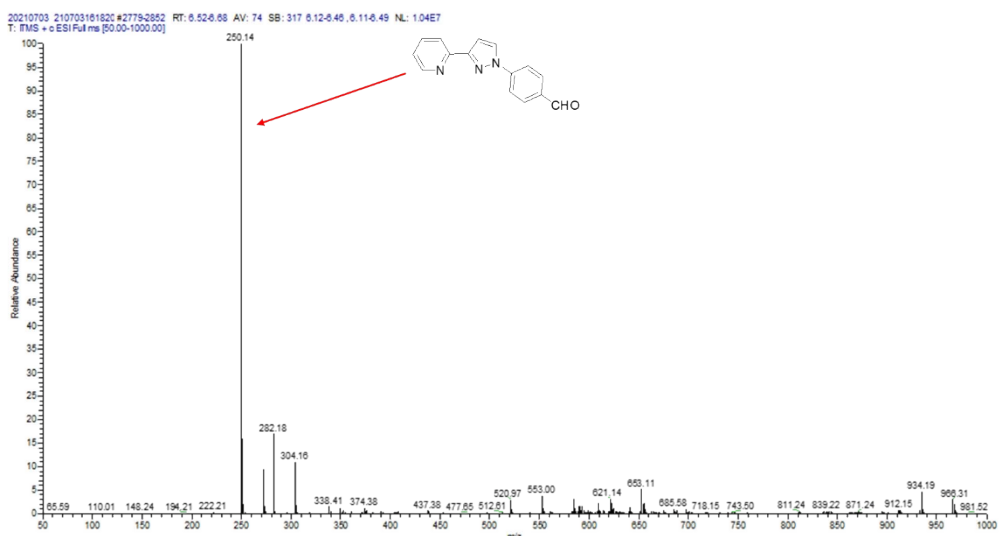


Fig. S2 ESI-MS spectrum, ^1H NMR spectrum of o-ppCHO

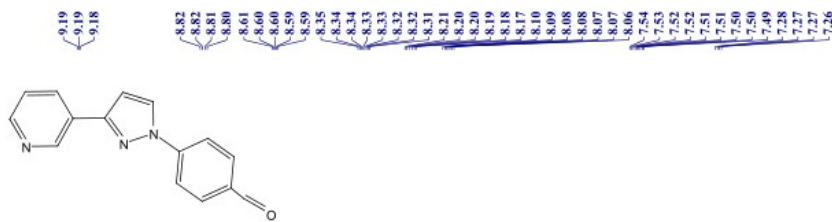
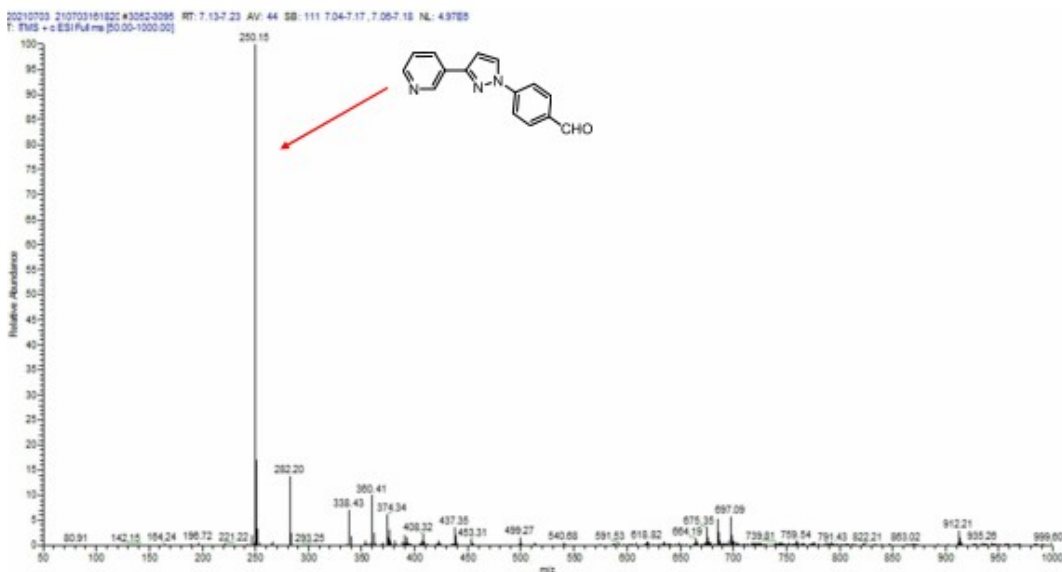


Fig. S3 ESI-MS spectrum, ^1H NMR spectrum of m-ppCHO

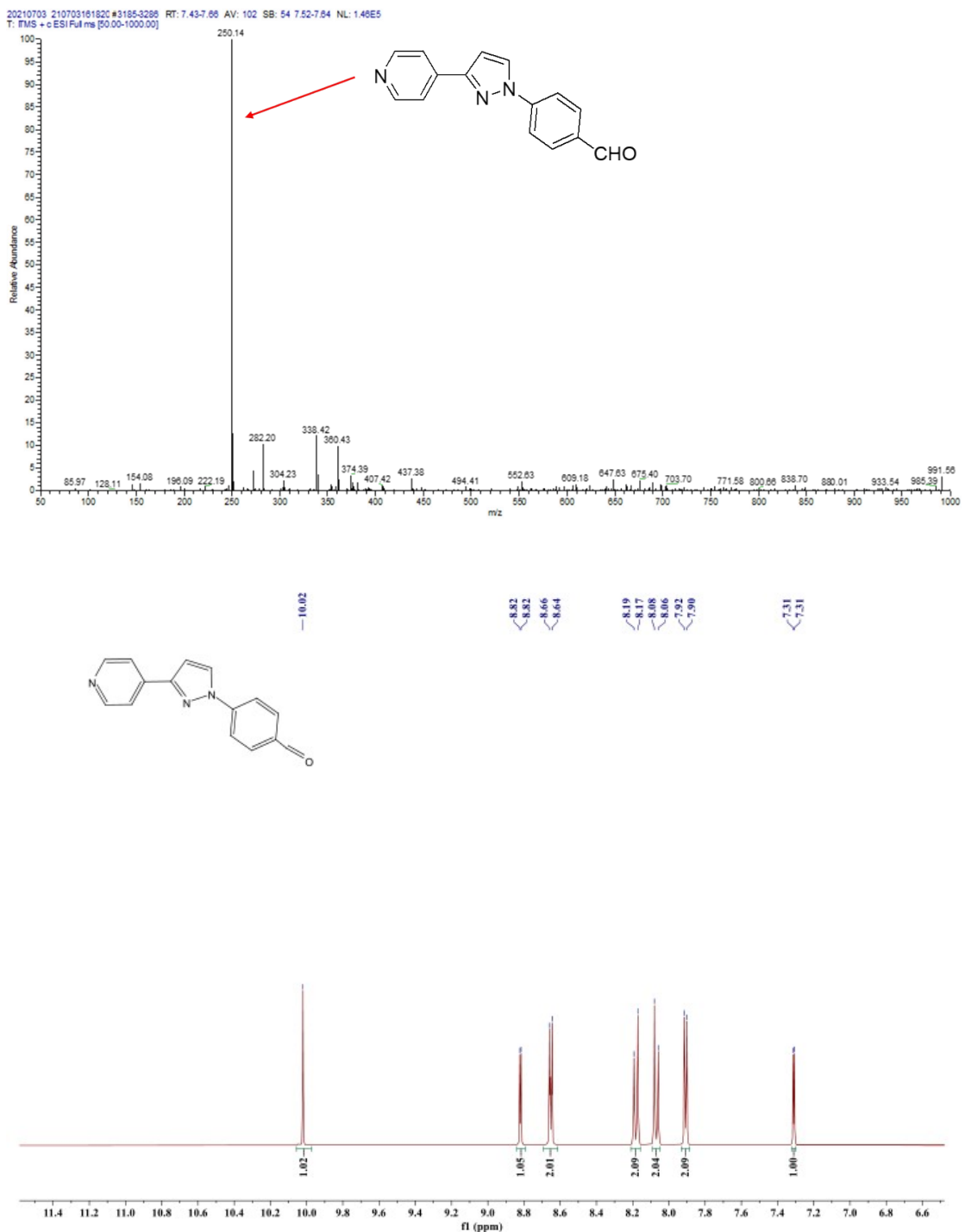


Fig. S4 ESI-MS spectrum, ^1H NMR spectrum of p-ppCHO

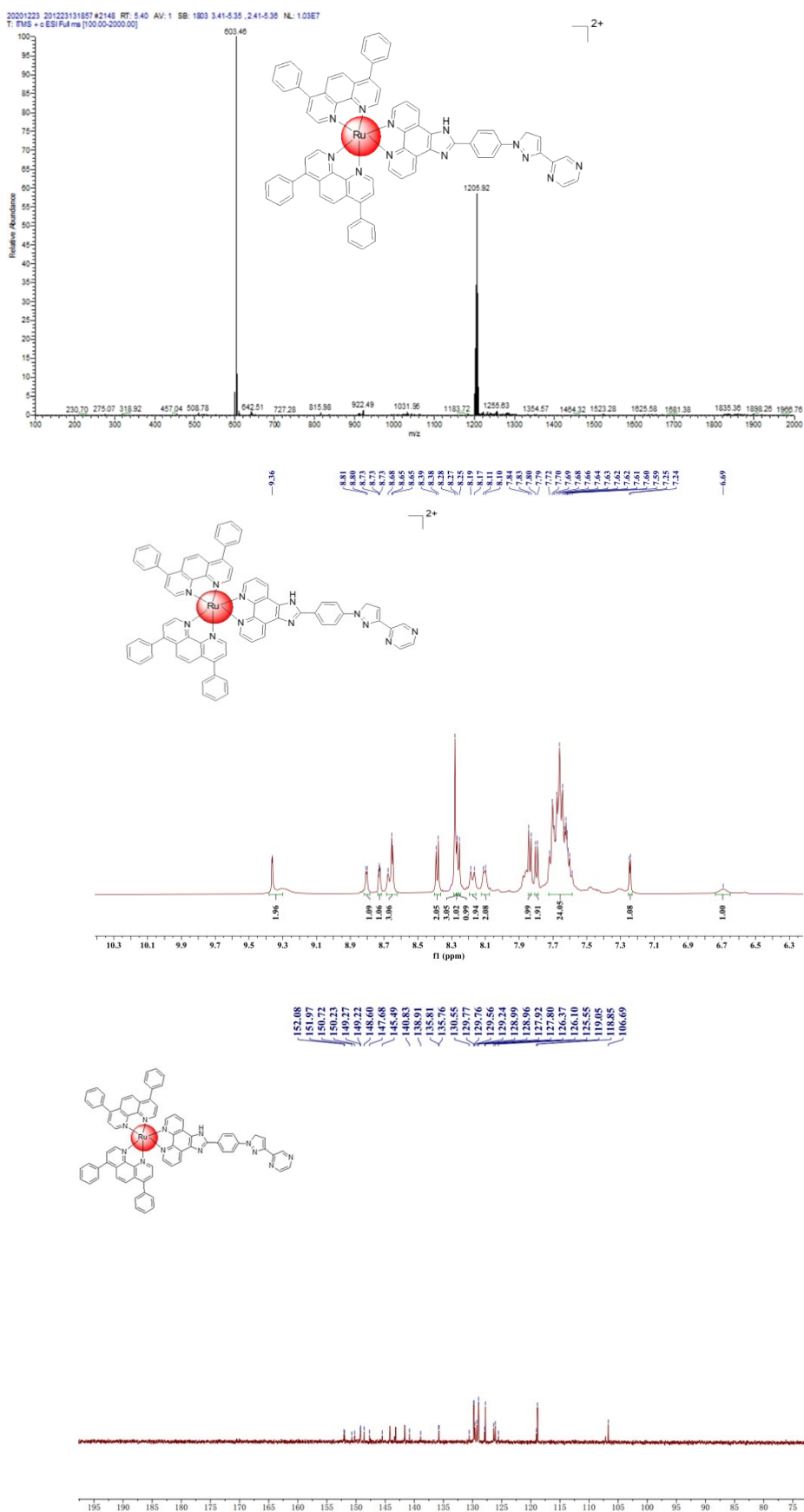


Fig. S5 ESI-MS spectrum, ^1H NMR(DMSO-d₆) and ^{13}C NMR (MeOD/DMSO-d₆ 6:1) spectrum of $\text{Ru}(\text{dip})_2(\text{o-pippz})^{2+}$

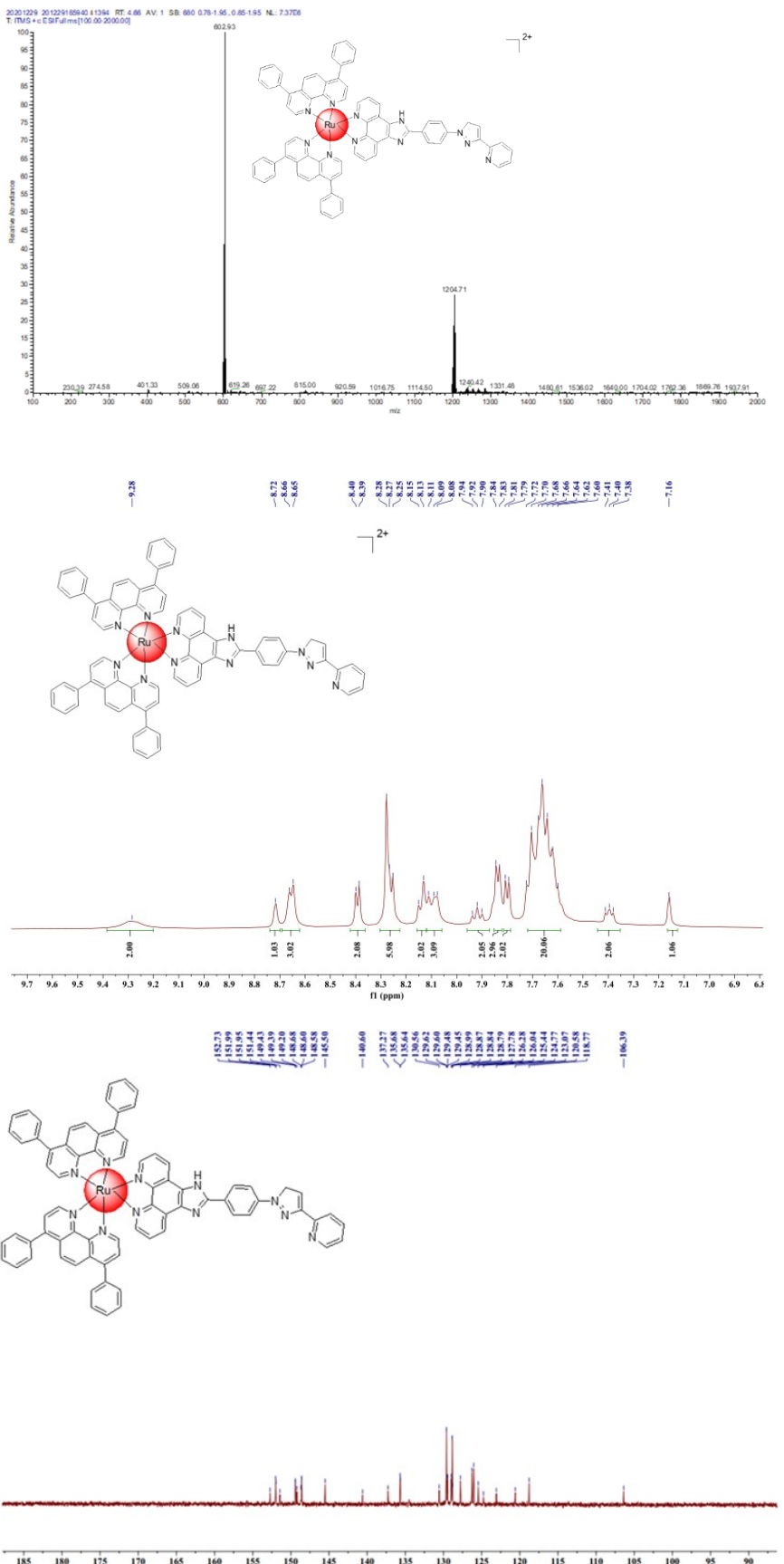


Fig. S6 ESI-MS spectrum, ^1H NMR (DMSO-d₆) and ^{13}C NMR(MeOD) spectrum of Ru(dip)₂(o-pipp)²⁺

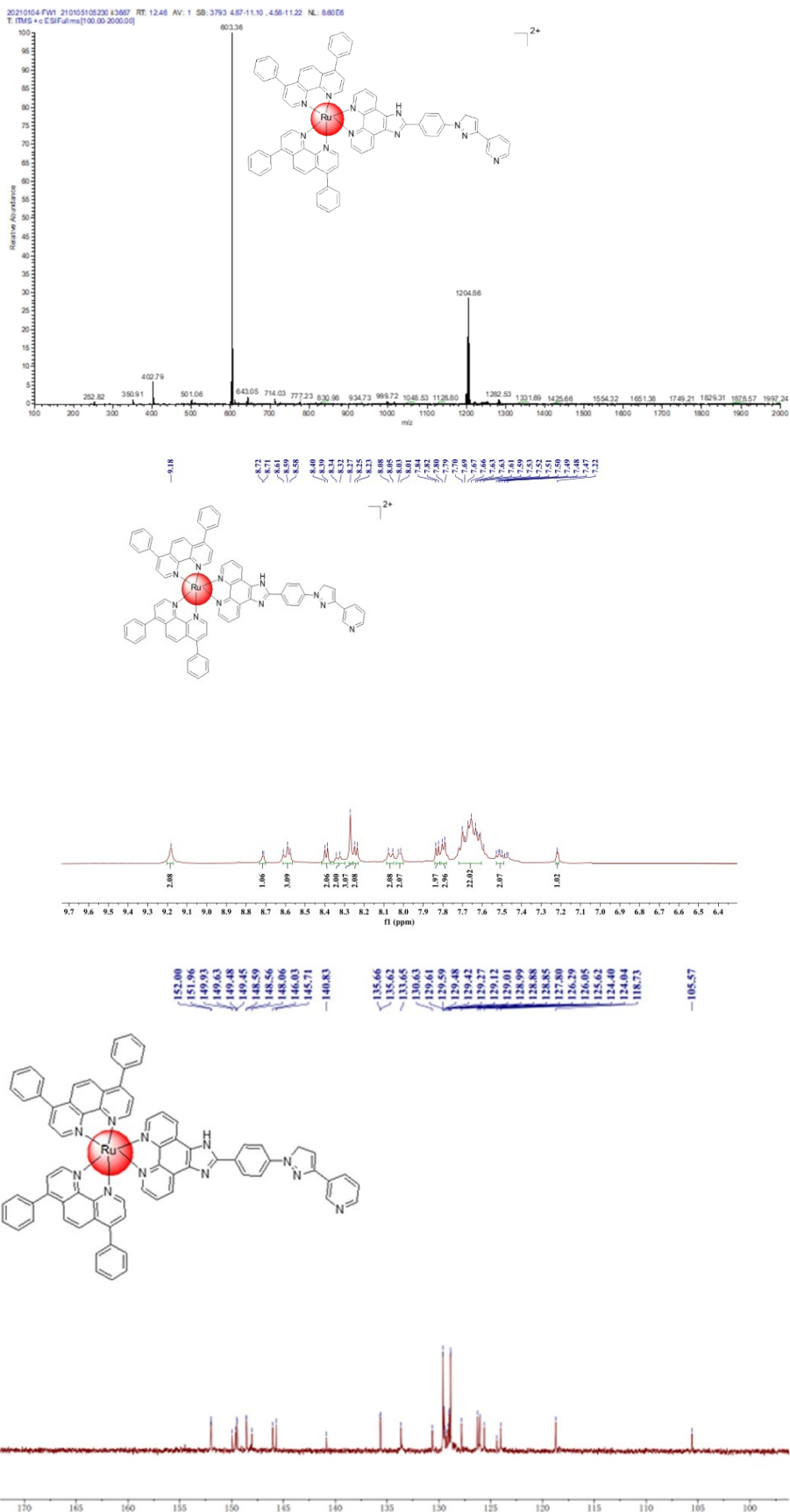


Fig. S7 ESI-MS spectrum, ¹H NMR (DMSO-d₆) and ¹³C NMR(MeOD) spectrum of Ru(dip)₂(m-pipp)²⁺

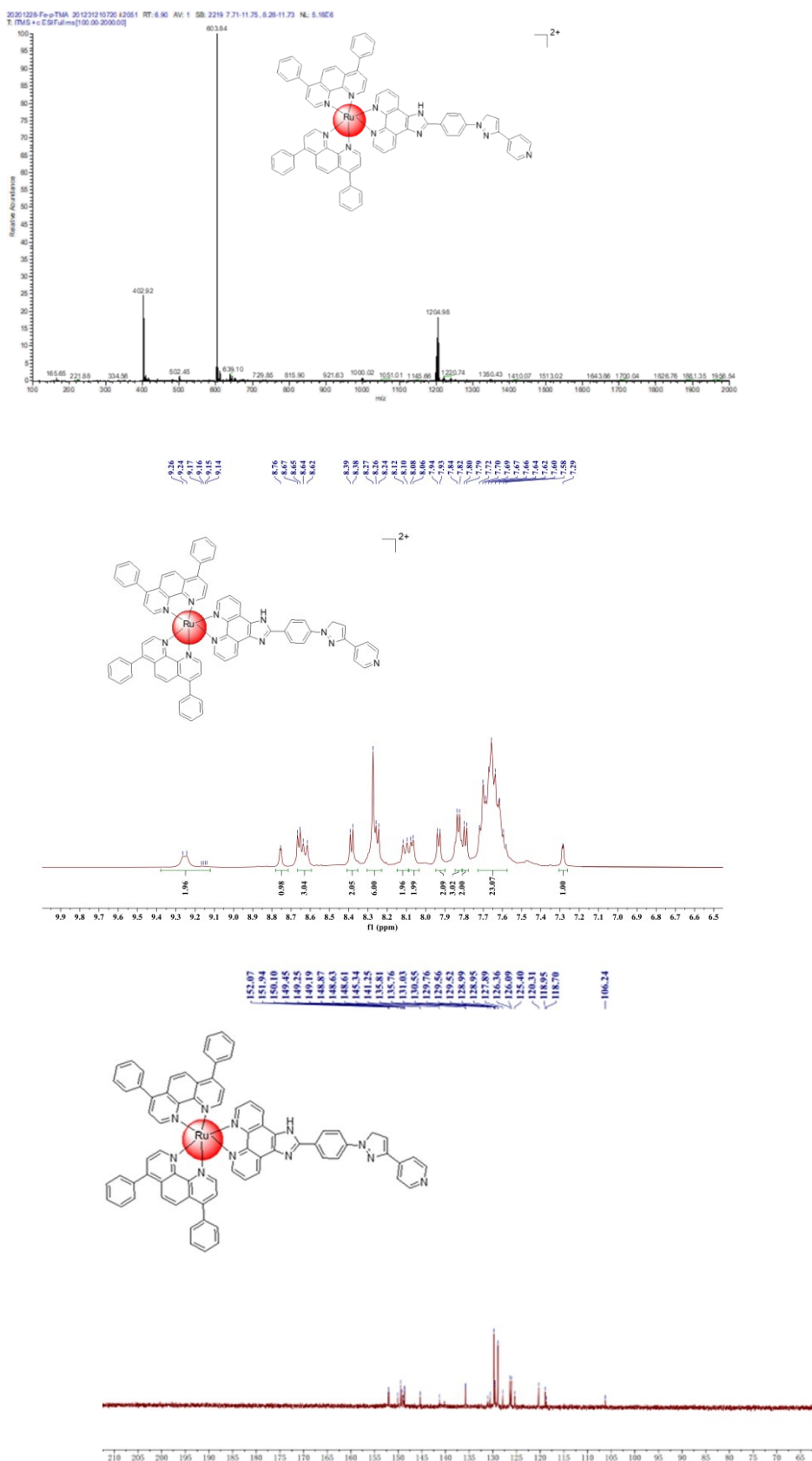


Table S1 Photophysical properties of Ru1-Ru4

complex	$\lambda_{\text{abs}}/\text{nm}(\log \epsilon)$	$\lambda_{\text{em}}/\text{nm}$	Φ_{em}	σ_2/GM
Ru1	445(2.92)	612	0.042	7
Ru2	465(3.11)	618	0.042	31
Ru3	465(3.08)	617	0.042	8
Ru4	465(3.18)	616	0.042	14

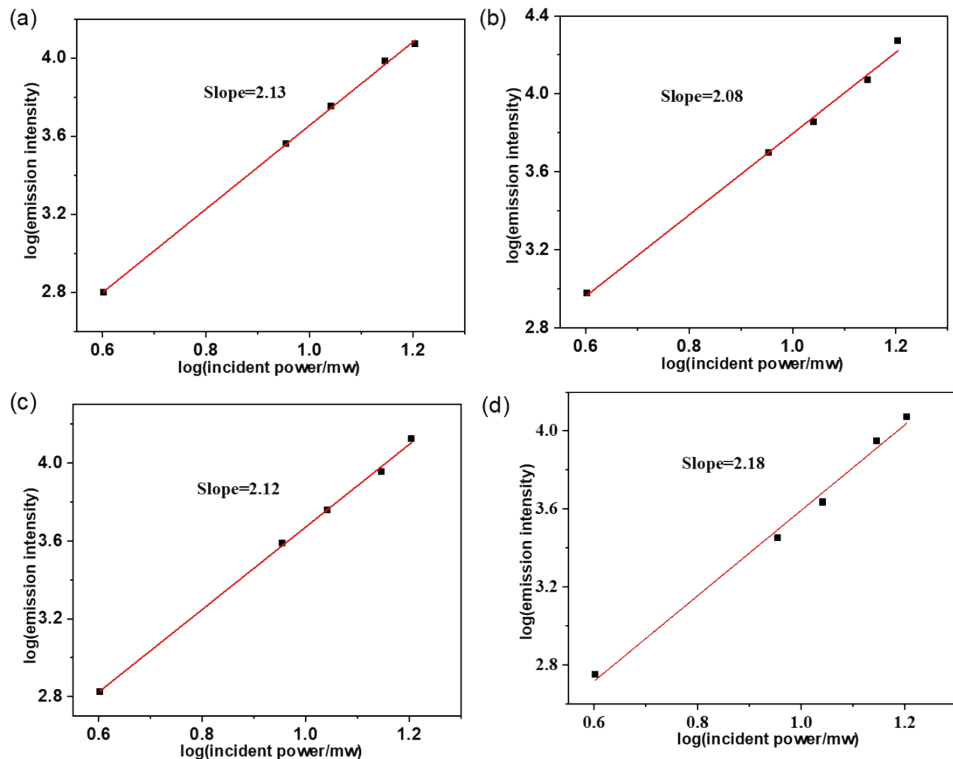


Fig. S9 The logarithmic plots of the power dependence of relative two-photon induced luminescence intensity of Ru1-Ru4 as a function of pump power at the optimal two-photon excitation wavelength. (a) Ru1 (b)Ru2 (c)Ru3 (d)Ru4

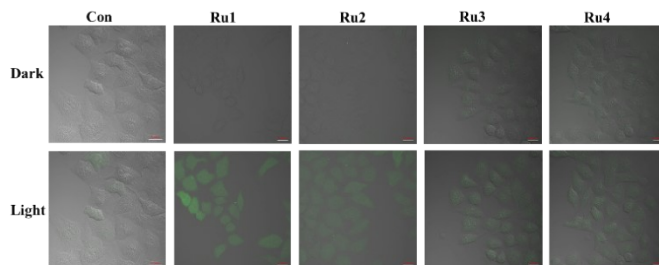


Fig. S10 Confocal images of HeLa before and after one-photon PDT Cells were preincubated for 10 h with DCFH-DA ($\lambda_{\text{em}} = 510-550 \text{ nm}$, $\lambda_{\text{ex}} = 488 \text{ nm}$) and Ru1-Ru4 (0.2 μM). scale bars = 100 μm

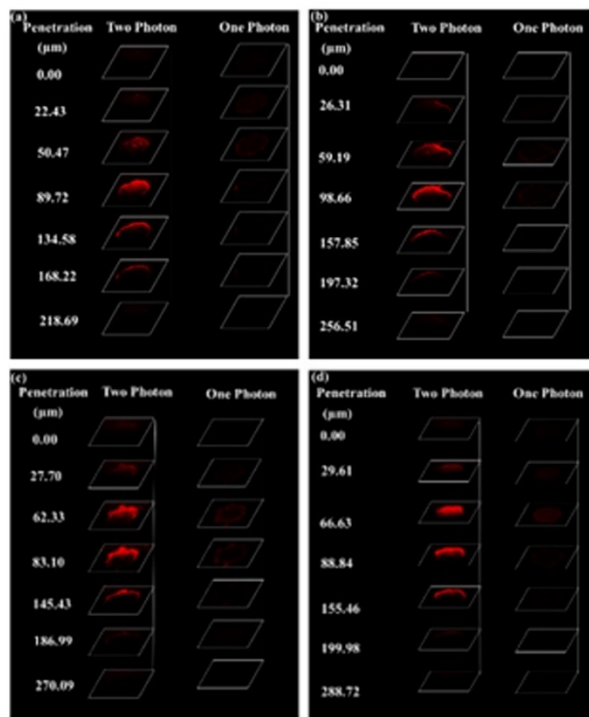


Fig. S11 MCSs were incubated with different concentration of Ru1-Ru4 for 10 h, followed by one-photon (OPM) and two-photon (TPM) Z-stack imaging microscopy (a) Ru1 (b) Ru2 (c) Ru3 (d) Ru4 .

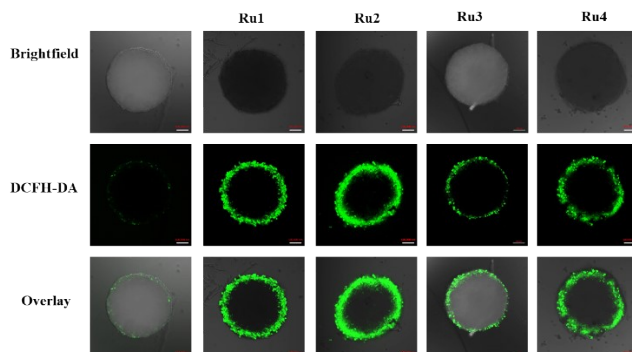


Fig. S12 DCFH-DA staining on pre-treated MCSs. The MCSs were incubated with 10 μM Ru-Ru4 and Control, respectively, for 10 h in the dark and subjected to 800 nm (Control)/810 nm (Ru1, Ru3)/820 nm (Ru2, Ru4) two-photon laser irradiations (100 mW, 1 kHz, 110 fs) for 3 m in per section in advance. scale bar = 200

References

1. R. Cano, D. J. Ramon and M. Yus, *J. Org. Chem.*, 2011, **76**, 654.